IEEE Transactions on Transportation Electrification, Available online 09 January 2023
DOI: 10.1109/TTE.2023.3235012

Efficient Mode Transition Control for DM-PHEV with Mechanical Hysteresis based on Piecewise Affine H_∞ Strategy

Cong Liang, *Student Member,* Xing Xu, *Member,* Daniel J. Auger, *Senior Member,* Feng Wang, and Shaohua Wang,

***Abstract*—A dual motor plug-in hybrid electric vehicle (DM-PHEVs) can achieve higher power and better fuel economy through Mode Transition Process (MTP) from pure electric to hybrid driving modes. In a DM-PHEV, the MTP is more complex, with more components to be managed. As well as being a combination of a discrete stage transition and a system with continuous state evolution, the several actuators exhibit significant discontinuous dynamics and different characteristics from each other, particularly mechanical hysteresis. This makes the design of a coordinated controller challenging. In this paper, a two-layer coordinated control strategy is proposed. The upper layer is based on a stage-dependent piecewise-affine (PWA) model which is used to develop a PWA-static output feedback H_∞ strategy (PWA-SOF). The lower layer is based on a simplified actuator lag model, and a H_∞ design technique is used to develop a robust torque controller that reduces the effect of mechanical hysteresis. The resulting strategy is described as a piecewise-affine modified static output feedback (PW-MSOF) algorithm. (While the individual elements are not novel contributions to control theory, the combination and application to this problem is.) Performance indices are defined and hardware-in-the-loop (HiL) test shows that the new controller can effectively suppress the vehicle jerk without adversely affecting other aspects of system behaviour.**

***Index Terms*—Mode transition process, PWA, Mechanical hysteresis, PHEV, H_∞**

I. Introduction

With the energy crisis and anthropogenic climate change presenting significant world challenges, the arguments for replacing conventional fossil-fuel vehicles are strong, and electric vehicles and hybrid electric vehicles (HEV) have become an attractive choice [1]. An HEV has multiple power sources, typically an internal combustion engine (ICE) and one or more motors, which enable an HEV to work in various operating modes. The choice of mode and the torque distribution between power sources is decided by an energy management controller (EMC) which usually aims for optimal long-term energy consumption. However, among the mode transitions are some highly nonlinear events such as engine start/off and clutch engagement/disengagement which may interrupt power or cause torque fluctuations. Also, the discontinuous characteristics of actuators may lead to vehicle jerk and which may transmit vibrations from actuators to the vehicle body, reducing passenger ride comfort. For the control designer, it is important to design a coordinated controller that reduces this to an acceptable level [2].

Numerous methods related to engine start, clutch engagement, torsional vibration elimination control strategy have been proposed to improve the performance of mode transition process (MTP). Engine start-up is an inevitable process during MTP. For PHEVs with engine directly connected to the input shaft, the drive-line oscillations are mainly caused by the engine ripple torque at low speed. Zhao et al. designed the optimal crank track for engine speed to start the engine smoothly and improve ride comfort [3]. Motors are usually used in this structure to compensate the abrupt change in engine output torque for its fast response speed [4]. For plug-in hybrid electric vehicles (PHEVs) with engine connected with power-train through a clutch, the engine can be started by the engagement of clutch. The performance of MTP is highly dependent on the control of clutch [5]. Zhou et al. proposed a linear quadratic regulator (LQR) coordinated controller considering both the vehicle jerk and clutch slipping energy loss to smoothly engage the clutch [6]. Xu et al. developed a coordinated dynamic surface control which considered uncertainties or disturbances of the system for the MTP of a power-split hybrid powertrain, and the vehicle jerk can be suppressed within $10\mathrm{m/s}^3$ with observer error of clutch oil pressure [7]. Besides the usual performance index, Wang et al. proposed an optimal oil-pressure curve which was optimized through considering the rotational displacement-based varying mesh stiffness (RDMS) of gear teeth and building a nonlinear transient torsional vibration (TTV) model of planetary hybrid power-split system (PHPS), both the TTV and ride comfort is enhanced through the oil-pressure optimization [8].

As the torque transmitted by clutch is different in clutch slipping stage and clutch engagement stage, which results in discontinuous dynamic characteristics in MTP with clutch engagement process [9]. Thus, Song et al. divided the switching process into three stages according to the vehicle dynamics, and different control strategies are proposed for each process [10]. However, switched control strategies during MTP may

Cong Liang, Xing Xu, Feng Wang and Shaohua Wang are with the Automotive Engineering Research Institute, Jiangsu University, Zhenjiang, China; Jiangsu Province Engineering Research Center of Electric Drive System and Intelligent Control for Alternative Vehicles, Zhenjiang 212013, China. e-mail: xuxing@ujs.edu.cn.

Cong Liang, Daniel J. Auger is with the School of Aerospace, Transport and Manufacturing, Cranfield University, College Road, Cranfield, Bedfordshire, MK43 0AL, U.K.

Corresponding author: Xing Xu

introduce instability into the MTP system and local controller can hardly acquire optimal results in global. PWA system provides a new possibility to describe the MTP system with discontinuous clutch engagement process. PWA define the state equation of nonlinear system into polyhedral region and associate each region a with different affine state update equation. It has been employed in the description of many fields, such as lateral tire forces [11], [12] and magneto-rheological (MR) suspension system [13]. Considering the time-varying load of suspension with physical constraints, Wu et al. proposed a parameter-dependent piecewise-quadratic Lyapunov function to design a load-dependent PWA H_∞ controller for the adjustment of MR dampers, the performance of suspension can be significantly improved [14], [15]. To suppress the driveline oscillations and improve passenger comfort, Constantin et al. used the PWA model to describe the the powertrain with dry clutch and proposed a predictive controller based on flexible Lyapunov functions [16]. Although PWA system has been widely used in the model of nonlinear and discontinuous systems, few contributions about the application of PWA to MTP with discontinuous clutch engagement process has been reported before.

Another important problem for MTP is the different response speed of actuators. The torque of motors and clutch need to change quickly to acquire a fast and smooth MTP. Many studies have been conducted to design the motor control strategy to improve the dynamic response of motors [17]–[19]. From the results of these studies, we can find that though a well-designed control strategy for motors can improve the response speed of motors, the response speed cannot be eliminated due to the physical limitations. Situations are even more serious in the control of wet clutch. Paul D.Walker et al. built detailed model of direct acting solenoid valves for clutch control, and experiments were conducted to verify the model, experiment results showed that the maximum hysteresis noticeable reached to 0.3 s because of the motion of the valve spool [20]. Jinrak Park et al. proposed an adaptive control method of the clutch torque in the slip engagement of a wet clutch to enhance the response speed of wet clutch, results of experiments verified that the response speed can be improved but cannot be eliminated [21]. It can be found that no matter how the controller of the lower actuator is improved, it always takes some time for the actuator to respond to the demand torque from the Hybrid Control Unit (HCU). And for hydraulically controlled clutches and current controlled motors, their response times are necessarily inconsistent. The hysteresis of the actual actuator torque compared to the demanded torque due to the physical properties of the actuator is the mechanical hysteresis studied in this paper. The key goal of MTP is coordinating the torque of actuators. The mechanical hysteresis of clutch is definitely much bigger than that of motor. The different response speed will result in uncoordinated dynamic torque of actuators, which deteriorate the performance of MTP. There is no doubt that the coordination between torque of motors and clutch cannot be realized in the Motor Control Unit (MCU) and Transmission Control Unit (TCU) separately. The only way to solve this problem is considering the mechanical hysteresis in the HCU. Some researches have been conducted to eliminate the inconsistent torque responses of actuators. Liu et al. took system dynamic characteristics into consideration and built detailed dynamic models for engine, clutch and motor of HEV, the comparison between simulation results of dynamic models and test data of bench test verified the effectiveness of proposed models [22]. However, the dynamic characteristics of actuators are not considered in the proposed coordinated control strategy. Yang et al. considered the different dynamic response of motor and hydraulic brake system during braking MTP to design a coordinated control strategy for HEV, the target brake torque of motor was restricted by the changing rate of hydraulic brake force, and simulation results verified that the proposed strategy can effectively reduce the vehicle jerk of MTP from 77.6 $\mathrm{m/s^3}$ to 4.06 $\mathrm{m/s^3}$ [23]. However, only the dynamic characteristics of hydraulic brake system was considered in the research, the response speed of motor was assumed as instant. Gao et al. considered the time-varying delay of clutch pressure control and introduced the adaptive Smith predictor to compensate the time delay of clutch torque. However, the coordination between motors and clutch are realized by the limitation of torque changing rate of clutch, which will prolong the time of MTP [24].

Though the MTP process has been studied widely, few people focus on the different response speed between motors and wet clutch, and many of them treated the motor as instant respond speed. Besides, most coordinated controllers divided the MTP process into several stages and designed separate controllers for each stage, which can hardly ensure the global optimization and stability of MTP system. To obtain a smooth and fast MTP for DM-PHEV with discontinuous clutch engagement process and mechanical hysteresis, this paper first proposes a PWA-modified static output feedback H_∞ coordinated control (PWA-MSOF) for MTP from electric driving mode to hybrid driving mode. The main contributions of this paper are summarized as follows.

1) Considering that the discrete engagement of clutch and continuous state transition of DM-PEHV can be described as a hybrid system, PWA model of MTP is firstly built, which can be useful for dealing with the discontinuous dynamic characteristics introduced by clutch engagement. Based on the PWA model of mode transition process, the global optimization and stability can be ensured with the proposed PWA-SOF controller. This is different from the existing coordinated controller for MTP which just divided the MTP into several stages and design separate controller for them.
2) The mechanical hysteresis caused by clutch and motors is described by first-order systems and the map of hysteresis parameters are built. Although some research has been done to solve the mechanical hysteresis of actuators, they usually assumed that the response speed of motor is instant. This paper considered the response speed of all the motors and clutches in the proposed controller, and robust H_∞ controller is adopted here to deal with the time-varied mechanical hysteresis.

This paper is constructed as follows.

- Section II describes the DM-PHEV and formulates the

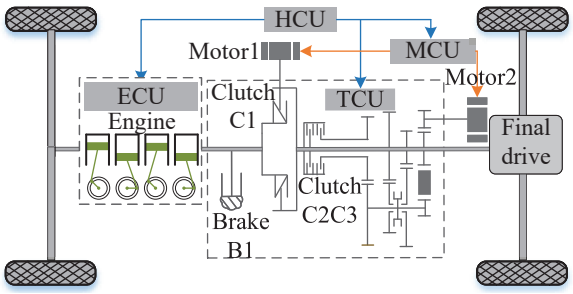

Fig. 1. Schematic diagram of the DM-PHEV.

MTP problem.

- Section III builts the PWA model of MTP
- Section IV identifies the mechanical hysteresis of actuators.
- Section V proposes the PWA-MSOF control strategy considering mechanical hysteresis of actuators to suppress the vehicle jerk.
- Section VI shows the simulation and HiL results.
- Section VII is the conclusion of this paper.

II. Problem Statement

A. Architecture of DM-PHEV

As shown in Fig.1, the architecture of vehicle is a DM-PHEV which includes an engine, two motors, three clutches and an automatic mechanical transmission (AMT), etc. Besides the normal driving motor which is named Motor 2, an additional Motor 1 is adopted in this structure to provide extra power and help adjust the working points of engine to obtain better fuel economy. Motor 2 is the drive motor and is primarily responsible for providing torque in electric driving mode. Clutch C1 is located between engine and motor 1. When the vehicle runs into hybrid driving mode, the clutch C1 should engage to couple the engine with the power-train. Through the engagement of Clutch C2&3, the powertrain system can switch different ratios. On the basis of control of clutches, the working modes of DM-PHEV can be switched. In this paper, the study focus on the engagement of clutch C1 to smoothly start the engine, various actuators in the structure will result in complicated coordination problem during the mode transition process.

B. Description of mode transition process

The MTP from electric driving mode (EM) to hybrid driving mode (HM) starts when the demand torque of vehicle, state of charge (SOC) of battery or vehicle speed exceeds the threshold determined by EMC strategy. The MTP from EM to HM can be divided into four stages as shown in Fig.2(a). The green dotted line represents the speed of the clutch driven disc ω_l. Different from the traditional internal combustion engine-driven vehicle, for the hybrid vehicle, the engine is started by the slipping of the clutch, so the clutch disc connected to the engine side is the driven disc. The solid purple line represents the speed of the clutch driving disc (the clutch disc connected to the powertrain) ω_r. Stage 1 is the electric driving stage,

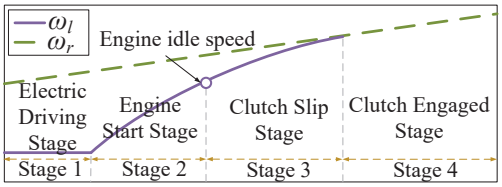

(a)

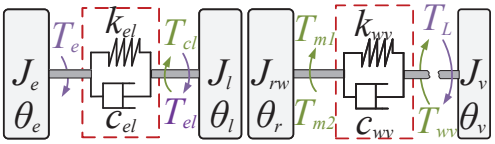

(b)

Fig. 2. (a)Mode transition process. (b)Model of DM-PHEV.

motor 2 drives the vehicle alone. If the mode transition order is given by EMC, the MTP system runs into engine start stage. Clutch C1 which is located between engine and motors begins to slip to start the engine during Stage 2. If the engine speed ω_e is greater than the engine idle speed ω_{eng_idle}, the MTP runs into Stage 3, clutch slip stage. As the torque of clutch T_{cl} transmitted to the driveline is resistance torque during the MTP. To avoid extra vehicle jerk, the torque of motors should provide extra torque to compensate the torque of clutch C1. Once the clutch engages, T_{cl} changes to the torque of engine T_e. If $T_e > 0$, the torque fluctuations will result in vehicle jerk. To avoid vehicle jerk at the end of Stage 3, the torque of engine T_e need to be zero during this stage and T_{cl} should be controlled to zero at the end of this stage. If the difference between the speed of clutch driving disc ω_r and the speed of clutch driven disc ω_l is smaller than a certain value ω_s, the clutch C1 engages and DM-PHEV runs into clutch engaged stage. The MTP completes and DM-PHEV can be driven by ICE and motors together.

III. PWA Model of DM-PHEV during MTP

A. Model of different stages of MTP system

As shown in Fig.2(b), based on the previous work [25], the simplified model of DM-PHEV during MTP for controller design can be described as:

$$\begin{aligned}
&T_e - J_e\ddot{\theta}_e = T_{el}, T_{el} = k_{el}\left(\theta_e - \theta_l\right) + c_{el}\left(\omega_e - \omega_l\right)\\
&T_{el} + T_{cl} = J_l\ddot{\theta}_l, -T_{cl} + T_{m1} + i_2 T_{m2} - \tfrac{T_{wv}}{i_0 i_g} = J_{rw}\ddot{\theta}_r\\
&T_{wv} = k_{wv}\left(\tfrac{\theta_r}{i_0 i_g} - \theta_v\right) + c_{wv}\left(\tfrac{\omega_r}{i_0 i_g} - \omega_v\right), T_{wv} - T_L = J_v\ddot{\theta}_v
\end{aligned} \tag{1}$$

with T_e being the torque of engine; J_e being the inertia moment of engine; θ_e being the angle of engine; k_{el} being the equivalent torsional stiffness of torsional damping spring; θ_l being the angle of clutch driven disc; c_{el} being the equivalent damping coefficient of torsional damping spring; ω_e being the speed of engine; ω_l being the speed of clutch driven disc; T_{cl} being the torque transmitted by clutch; J_l being the inertia moment of clutch driven disc; T_{m1} being the torque of motor 1; T_{m2} being the torque of motor 2; i_2 being the gear ratio of motor 2; i_0 being the final drive ratio; i_g

being the gear ratio of transmission; J_{rw} being the equivalent inertia moment of transmission; θ_r being the angle of clutch driving disc; θ_v being the angle of tire; ω_r being the speed of clutch driving disc; ω_v being the speed of tire; k_{wv} being the equivalent torsional stiffness of tire and half shaft; c_{wv} being the equivalent damping coefficient of tire and half shaft; J_v being the inertia moment of vehicle body; T_L being the resistance torque of vehicle.

The torque T_{cl} transmitted by the clutch can be described as a piece-wise model related to the clutch state:

$$T_{cl} = \begin{cases} 0 & \text{disengaged} \\ \mu R_m N A P_{cl} sign(\Delta w_c) & \text{slipping} \\ T_{lock} & \text{engaged} \end{cases} \tag{2}$$

with μ being the friction coefficient, R_m being the equivalent radius, N being the number of plates, A being the clutch pressure area, P_{cl} being the clutch pressure, Δw_c being the speed difference between the discs of clutch, T_{lock} being the input torque transmitted by the shaft. When the clutch is slipping, the torque transmitted by clutch can be controlled by the oil pressure; When the clutch is engaged, the torque transmitted by it will be related to the input torque. In this structure, the engaged clutch will transmit the torque of engine.

The state variables and control variables are selected as

$$\begin{aligned} x = &\left[\begin{array}{cccc} \theta_e - \theta_l & \omega_e & \omega_l - \omega_r & T_{cl} \\ \frac{\theta_r}{i_g i_0} - \theta_v & \omega_r & \omega_v & T_m - T_{cl} \end{array} \right]^T, u = \left[\begin{array}{c} \dot{T}_{cl} \\ \dot{T}_m \end{array} \right] \end{aligned} \tag{3}$$

For engine start stage and clutch slipping stage, the only difference in the model is the torque of engine T_e. During engine start stage, T_e represents the engine ripple torque before the spark ignites. After the engine starts, the torque of engine can be controlled by the Engine control Unit (ECU). Since the engine torque can be treated as output disturbance, the model of these two stages can be unified as:

$$\begin{cases} \dot{x} = A_1 x + B_1 u + d_1 \\ d_1 = \left[\begin{array}{cccccccc} 0 & T_e/J_e & 0 & 0 & 0 & 0 & -T_L/J_v & 0 \end{array} \right]^T \end{cases} \tag{4}$$

The boundary condition for these two stages can be described as $\omega_r - \omega_l \geq \omega_s$.

If $\omega_r - \omega_l \leq \omega_s$, the MTP runs into clutch engagement stage, the torque of clutch changes as described in Eq.(2). The model of MTP in this stage can be described as:

$$\begin{cases} \dot{x} = A_2 x + B_2 u + d_2 \\ d_2 = \left[\begin{array}{cccccccc} 0 & 0 & 0 & 0 & 0 & 0 & -T_L/J_v & 0 \end{array} \right]^T \end{cases} \tag{5}$$

The coefficient matrices of state space equations are shown in Table.I.

B. Piecewise affine model of MTP system

According to Eq.(2), the torque transmitted by clutch changes with the state of clutch, which results in different models for different stages of MTP. Due to the discontinuities introduced by clutch engagement, the model of the MTP system changes with the stage. In normal situations, individual controllers will be designed for each stage. However, the separate controllers can only ensure the stability and performance based on the model in one stage. The stability of transition between these stages and the global performance can hardly be optimized. Thus, a type of hybrid system, PWA system is adopted here to describe the MTP with discrete transition between these stages. The PWA model of MTP can be described as:

$$\dot{x} = A_i x + B_i u + d_i, x \in \Re_i \tag{6}$$

where $\Re_i = \{l_i \leq \omega_r - \omega_l \leq u_i\}$ is the i-th region of state variables. The state variables of MTP are divided into two regions. The upper limits u_i and lower limits l_i for each region are:

$$l_1 = \omega_s, u_1 = \omega_{\max}, l_2 = -\omega_s, u_2 = \omega_s \tag{7}$$

The control goal of MTP is to start the engine by controlling the slipping of the clutch and then engage the clutch smoothly. The control of MTP can be transformed into a reference speed tracking problem for the clutch plates. Since the control theory of the piecewise affine system is based on the zero point of the equilibrium point, it is necessary to translate the coordinates of the equilibrium point of MTP to the origin through coordinate transformation. When the system reaches equilibrium, the clutch engagement is completed and the speed at both ends of the clutch tracks the reference speed smoothly. The equilibrium point of the MTP system is $\dot{x} = 0$, then the equilibrium point of the state variables and the control variables of the system can be described as:

$$\begin{aligned} x^* = &\left[\begin{array}{cccc} -\frac{J_e a_{ref}}{k_{el}} & \omega_{ref} & 0 & 0 \\ \omega_{ref} & \frac{\omega_{ref}}{i_g i_0} & (J_e + J_{lw}) a_{ref} + \frac{T_L i_g i_0 + J_v a_{ref}}{{i_0}^2 {i_g}^2} & \end{array} \right]^T \\ u^* = &\left[\begin{array}{cc} 0 & \frac{B_a a_{ref}}{i_0 i_g} \end{array} \right] \end{aligned} \tag{8}$$

with B_a being the fitting coefficient of the square of vehicle speed; a_{ref} being the reference acceleration; ω_{ref} being the reference speed of clutch discs. The reference acceleration and reference angular speed can be calculated through the demand vehicle speed from driver as:

$$\omega_{ref} = \frac{v_{ref}}{R_t}, a_{ref} = \dot{\omega}_{ref} \tag{9}$$

There is no doubt that the equilibrium point exists in the clutch engagement stage. Thus, we can acquire the following equation:

$$\dot{x}^* = A_2 x^* + B_2 u^* + d_2 \tag{10}$$

Let $x = x_t + x^*, u = u_t + x^*$, the system obtained by translating the coordinates of the MTP system to (x^*, u^*) is:

$$\begin{aligned} &\dot{x}_t = A_i x_t + B_i u_t + (d_i - d_2) + (A_i - A_2) x^* \\ &+ (B_i - B_2) u^*, S_i = \{x_t \,|l_i - c x^* \leq c x_t \leq u_i - c x^* \} \end{aligned} \tag{11}$$

for $x_t \in S_i, i \in \{1, 2\}$.

External input and disturbance w are selected as:

$$w = \left[\begin{array}{ccc} d_w & T_e & \Delta B_a \end{array} \right]^T \tag{12}$$

where d_w represents the measurement noise and external disturbance in system; ΔB_a is the change of air resistance torque caused by change of vehicle speed.

TABLE I
COEFFICIENT MATRICES OF MTP SYSTEM

Stage	Coefficient Matrix
2&3	$A_1 = \begin{bmatrix} 0 & 1 & -1 & 0 & 0 & -1 & 0 & 0 \\ -k_{el}/J_e & -c_{el}/J_e & c_{el}/J_e & 0 & 0 & c_{el}/J_e & 0 & 0 \\ k_{el}/J_l & c_{el}/J_l & -c_{el}/J_l & 1/J_l & k_{wv}/(J_{rw}i_0i_g) & c_{wv}/(J_{rw}{i_0}^2{i_g}^2) - c_{el}/J_l & -c_{wv}/(i_0i_gJ_{rw}) & -1/J_{rw} \\ 0 & 0 & 0 & 0 & 0 & 0 & 0 & 0 \\ 0 & 0 & 0 & 0 & 0 & 1/(i_0i_g) & -1 & 0 \\ 0 & 0 & 0 & 0 & -k_{wv}/(J_{rw}i_0i_g) & -c_{wv}/(J_{rw}{i_0}^2{i_g}^2) & c_{wv}/(i_0i_gJ_{rw}) & 1/J_{rw} \\ 0 & 0 & 0 & 0 & k_{wv}/J_v & c_{wv}/(J_vi_0i_g) & -c_{wv}/J_v & 0 \\ 0 & 0 & 0 & 0 & 0 & 0 & 0 & 0 \end{bmatrix}$ $B_1 = \begin{bmatrix} 0 & 0 & 0 & 1 & 0 & 0 & 0 & -1 \\ 0 & 0 & 0 & 0 & 0 & 0 & 0 & 1 \end{bmatrix}^T, E_1 = \begin{bmatrix} 0 & 0 & 1 & 1 & 0 & 1 & 0 & 1 \\ 0 & 1/J_e & 0 & 0 & 0 & 0 & 0 & 0 \\ 0 & 0 & 0 & 0 & 1/k_{wv} & 0 & 1/J_v & 1/i_0i_g \end{bmatrix}^T$
4	$A_2 = \begin{bmatrix} 0 & 1 & 0 & 0 & 0 & -1 & 0 & 0 \\ -k_{el}/J_e & -c_{el}/J_e & 0 & 0 & 0 & c_{el}/J_e & 0 & 0 \\ 0 & 0 & 0 & 0 & 0 & 0 & 0 & 0 \\ 0 & 0 & 0 & 0 & 0 & 0 & 0 & 0 \\ 0 & 0 & 0 & 0 & 0 & 1/(i_0i_g) & -1 & 0 \\ k_{el}/J_{lw} & c_{el}/J_{lw} & 0 & 0 & -k_{wv}/(J_{lw}i_0i_g) & -c_{wv}/(J_{lw}{i_0}^2{i_g}^2) - c_{el}/J_{lw} & c_{wv}/(i_0i_gJ_{lw}) & 1/J_{lw} \\ 0 & 0 & 0 & 0 & k_{wv}/J_v & c_{wv}/(J_vi_0i_g) & -c_{wv}/J_v & 0 \\ 0 & 0 & 0 & 0 & 0 & 0 & 0 & 0 \end{bmatrix}$ $B_2 = \begin{bmatrix} 0 & 0 & 0 & 1 & 0 & 0 & 0 & 0 \\ 0 & 0 & 0 & 0 & 0 & 0 & 0 & 1 \end{bmatrix}^T, E_2 = \begin{bmatrix} 0 & 0 & 0 & 0 & 0 & 1 & 0 & 1 \\ 0 & 0 & 0 & 0 & 0 & 0 & 0 & 0 \\ 0 & 0 & 0 & 0 & 1/k_{wv} & 0 & 1/J_v & 1/i_0i_g \end{bmatrix}^T$

Finally, we can acquire the standard PWA model of mode transition process as:

$$\begin{aligned} &\dot{x}_t = A_i x_t + B_i u_t + E_i w + b_i \\ &b_i = (A_i - A_2)\, x^* + (B_i - B_2)\, u^*, x_t \in S_i \end{aligned} \tag{13}$$

As the model built in this section is used for the design of coordinated controller which works on discrete frequency, the state space equation built before should be discretized. Then, the model of MTP including the change of torque transmitted by clutch can be transformed as a class of discrete-time PWA systems [13]:

$$\begin{cases} x_t(k+1) = A_i^d x_t(k) + B_i^d u_t(k) + E_i^d w(k) + b_i^d \\ A_i^d = e^{A_i T_s}, B_i^d = \int_0^{T_s} e^{A_i(T_s - x)} B_i dx \\ E_i^d = \int_0^{T_s} e^{A_i(T_s - x)} E_i dx, b_i^d = \int_0^{T_s} e^{A_i(T_s - x)} b_i dx \end{cases} \tag{14}$$

where $x_t(k)$ is the system state vector; $w(k)$ is the disturbance input vector which belongs to $l_2[0, \infty)$; A_i, B_i are the system matrices with corresponding dimensions of the ith subsystem.

Remark 1. For normal PWA system, the system region partitions can be divided into two classes $\Gamma = \Gamma_0 \cup \Gamma_1$, where Γ_0 is the set which contains origin-included partitions, and Γ_1 is the set of the origin-excluded partitions [26]. For the MTP system of DM-PHEV, the model changes with the state of clutch. The inequality to describe the border of regions can be rewritten as:

$$\begin{bmatrix} x_t \\ 1 \end{bmatrix}^T \begin{bmatrix} {H_i}^T H_i & * \\ {h_i}^T H_i & {h_i}^T h_i - 1 \end{bmatrix} \begin{bmatrix} x_t \\ 1 \end{bmatrix} \le 0 \tag{15}$$

where

$$\begin{aligned} &H_i = 2c/(u_i - l_i), h_i = (2cx^* - u_i - l_i)/(u_i - l_i) \\ &c = \begin{bmatrix} 0 & 0 & 1 & 0 & 0 & 0 & 0 & 0 \end{bmatrix} \end{aligned} \tag{16}$$

Remark 2. Let $\Theta = \{(i,j) \,|x_t(k) \in S_i, x_t(k+1) \in S_j\}$ represents the set of index pairs which denotes the possibility of switching from one partition to others or itself [27]. The possible switch of MTP system can be divided into three conditions: the state variables transit in the region of Stage 2/3; the state variables transit from the region of Stage 2/3 to the region of Stage 4; the state variables transit in the region of Stage 4.

The performance indices which can be used to evaluate the MTP include:

1) Optimal ride comfort: One of the most important index is to insure the ride comfort of passengers, which can be evaluated by the vehicle jerk $\min j = \min \dot{a} = \min \ddot{v}$, with a being the longitudinal acceleration of vehicle.
2) Minimum energy consumption: The slip of clutch may cause extra energy consumption, and this can be expressed as the clutch slipping energy loss $\min W = \min \int_{t_0}^{t_f} T_{cl}(\omega_l - \omega_r) dt$.
3) Torque demand of driver: Torque demand is expressed as the tracking of the driver's desired speed $\min(\omega_r - \omega_{ref})$.

Considering the performance indices of MTP, the performance outputs z are selected as:

$$\begin{aligned} z = \Big[\; & \omega_l - \omega_{cr} \quad T_{cl} \quad \dot{T}_{cl} \quad \omega_r - \omega_{ref} \\ & T_m - T_{cl} - (J_e + J_{lw})\, a_{ref} - \tfrac{T_L i_g i_0 + J_v a_{ref}}{{i_0}^2 {i_g}^2} \quad \dot{T}_m - \tfrac{\dot{T}_{cl}}{i_2} \Big]^T \end{aligned} \tag{17}$$

The performance output $\omega_l - \omega_r$ is selected to start the engine quickly and engage the clutch smoothly; T_{cl} is selected to ensure the minimum energy consumption, the torque transmitted by the clutch at the end of the slipping stage is expected to be zero to avoid the sudden change of torque; $\dot{T}_{cl}$ is selected to limit the sudden change of wet clutch; $\omega_r - \omega_{ref}$ is selected to meet the torque demand of driver; $T_m - T_{cl} - J_{ew} - \frac{T_L i_g i_0 + J_v a_{ref}}{{i_0}^2 {i_g}^2}$ is also selected to minimum

the energy consumption of motors; $\dot{T}_m - \frac{\dot{T}_{cl}}{i_2}$ is selected to ensure the coordination between torque of clutch and motors.

Since the angle signals in the state variables are difficult to be measured directly by the sensor, the measurement output y of the system is defined as:

$$\begin{aligned} y = \Big[& \omega_l - \omega_{cr} \quad T_{cl} \quad \omega_r - \omega_{ref} \\ & T_m - T_{cl} - (J_e + J_{lw})\, a_{ref} - \tfrac{T_L i_g i_0 + J_v a_{ref}}{{i_0}^2 {i_g}^2} \Big]^T \end{aligned} \tag{18}$$

Finally, the PWA model of MTP system can be written as:

$$\begin{cases} x_t(k+1) = A_i^d x_t(k) + B_i^d u_t(k) + E_i^d w(k) + b_i^d \\ z\,(k) = C_i x_t(k) + D_i u_t(k), y\,(k) = C_i^y x_t(k) \end{cases} \tag{19}$$

IV. Identification of Mechanical Hysteresis

The PWA model of MTP built above assumes that the torque of actuators can response the command of controllers immediately. However, once the torque command is given by the coordinated controller, it takes a little time for the controllers of actuators to adjust the actual torque of actuators to the desired torque. To describe the actual response of actuators, the mechanical hysteresis identification of the clutch and the motor is carried out in this section. As both the clutch and motors have its own controllers, the characteristics of mechanical hysteresis are influenced by the controllers of actuators. The identification of mechanical hysteresis is based on actuators with fixed controllers.

A. Mechanical hysteresis of wet clutch control system

To simulate the dynamic characteristics of the wet clutch, an electro-hydraulic system from proportional valve current to clutch friction torque is established. Here the model of electro-hydraulic system is built according to [7]. Based on the AMESim model of wet clutch, the step response of wet clutch is simulated as shown in Fig.3. Fig.3(a) is the torque response of wet clutch under constant current. It can be found that the hydraulic system of wet clutch result in sever hysteresis. Besides, we can find that the current-steady torque curve in Fig.3(b) shows dead zone at small current and pressure saturation at big current. The nonlinear dynamics of electro-hydraulic system makes it difficult to design the controller of wet clutch system. Thus, the stable torque response of wet clutch is fitted by a third-order polynomial T_{cl}-I curve as shown in Fig.3(b).

$$T_{cl} = p_1 I^3 + p_2 I^2 + p_3 I + p_4 \tag{20}$$

where

$$p_1 = -0.000384, p_2 = 0.05614, p_3 = 3.971, p_4 = -88.26 \tag{21}$$

with I being the current of the proportional valve.

As the controller of electro-hydraulic system is not the key problem of this paper, based on the fitting curve in Fig.3(b), a PID controller in [7] is adopted here to control the current of valve to adjust the actual torque of clutch to the torque demand T_{cl_dmd} from upper controlle as shown in Fig.3(c).

The mechanical hysteresis of wet clutch is inexorable inherent characteristics.

In order to compensate for the vehicle jerk caused by dynamic characteristics of actuators in the coordinated controller, a simplified model must be constructed to describe the mechanical hysteresis. It can be seen from Fig.3 that the dynamic response of clutch is similar to the first-order system, To describe the mechanical hysteresis in simplified mathematical model, a first-order system is adopted here as:

$$\tau_{cl} \frac{dT_{cl}\,(t)}{dt} + T_{cl}\,(t) = u_{cl}\,(t) \tag{22}$$

with τ_{cl} being the hysteresis parameter of clutch, u_{cl} being the reference torque demand of clutch.

Curve fitting tool of MATLAB is used here to fit the delay parameter τ_{cl} in Eq.(22). From the simulation results we can find that τ_{cl} may vary with the initial torque and final demand torque, the final results τ_{cl} is shown in Fig.3(d).

To verify the accuracy of fitting, here a step response of wet clutch control system is shown in Fig.3(e) as a example. We can find that the reference torque is 80 Nm, the real torque transmitted by clutch experiences a dead zone and then acts as a one-order response. It can be seen that though the fitting torque does not perfectly fit the actual torque of the clutch, but compared with the demand torque given by the controller, the error between the fitted dynamic torque and the actual torque is smaller. Various step torque demand orders are give to wet clutch, and the errors between actual torque and fitting torque of wet clutch are shown in Fig.3(f). The fitting torque according to Eq.(22) can effectively eliminate the error between demand torque and real torque transmitted by clutch. Thus, Eq.(22) can be used to model the dynamic characteristics of wet clutch system.

B. Mechanical hysteresis of PMSM control system

Similarly, proportional–integral–derivative (PID) control strategy is adopted here as the controller of motors [28]. The plant model of PMSM and its controller can be built by the commercial software AMESim. Based on the simulation results of AMESim, we can find that the actual motor torque shows hysteresis relative to the demand motor torque as shown in Fig.4(a). Besides, the hysteresis varies with the range of torque demand. Thus, here a first-order system is also adopted here to model the mechanical delay exists in motor control system as

$$\tau_m \frac{dT_m\,(t)}{dt} + T_m\,(t) = u_m\,(t) \tag{23}$$

with τ_m being the hysteresis parameter of motors, u_m being the reference torque demand of motor.

Using the curve fitting tool of MATLAB we can acquire a map of hysteresis parameter τ_m of motor control system as shown in Fig.4(b). We can find that the mechanical hysteresis of motor system ranges from about 1 ms to 6.3 ms. The value is related to the initial motor torque and final demand torque.

To verify the effectiveness of model of dynamic response characteristics, the fitted torque under the demand torque of 80Nm is compared with the actual motor torque, as shown in

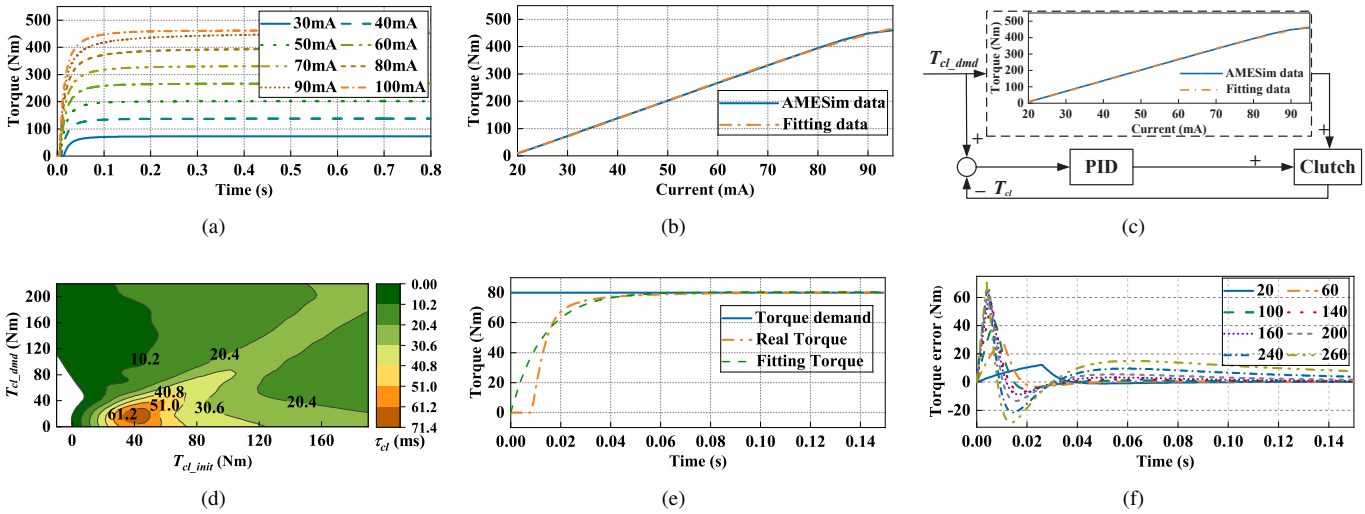

Fig. 3. Dynamic characteristics of wet clutch. (a)Response characteristics of wet clutch C1. (b)Current-Torque fitting curve. (c)Control strategy of clutch. (d)Mechanical hysteresis of clutch. (e)Torque comparison of clutch. (f)Torque error comparison of clutch.

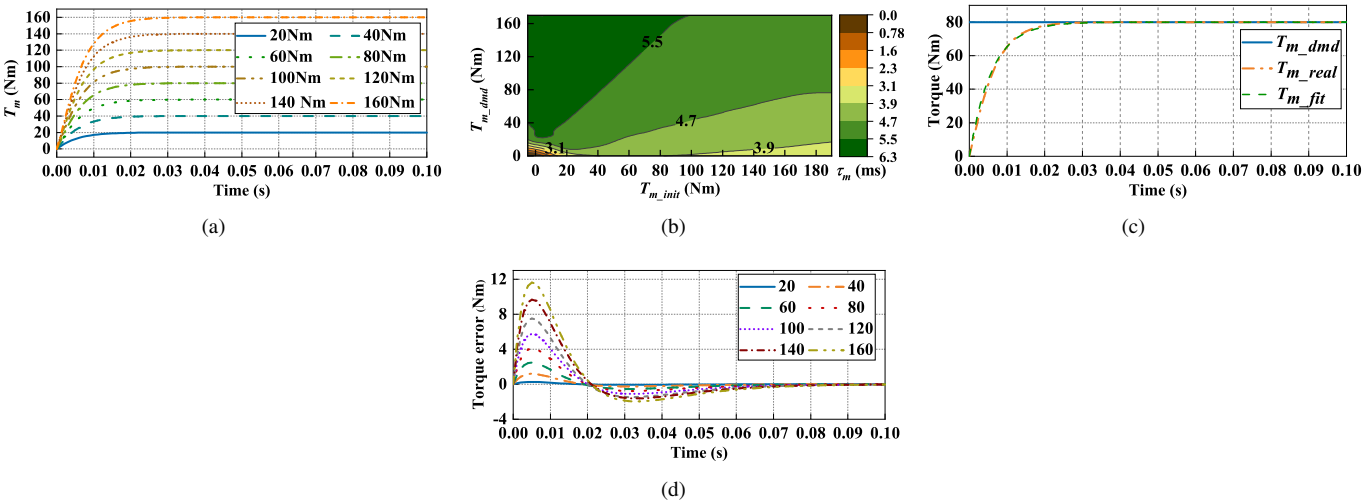

Fig. 4. Dynamic characteristics of PMSM. (a)Response characteristics of PMSM. (b)Mechanical hysteresis of PMSM. (c)Torque comparison of PMSM. (d)Torque error comparison of PMSM.

Fig.4(c). It can be found that the fitting torque is closed to the real torque of PMSM.

Besides, the error between fitting torque and real torque under different demand torque are simulated and the results are shown in Fig.4(d), the maximum error between fitting torque T_{m_fit} and actual motor torque is only 12 Nm at a step torque demand of 120 Nm.

Thus, the proposed dynamic model in Eq.(23) can effectively describe the dynamic response of motor control system.

The simplified model of MTP system with hysteresis built in this section is the preparation for the coordinated controller which will be designed in the next section.

V. PWA-MSOF H_∞ COORDINATED CONTROL STRATEGY CONSIDERING MECHANICAL HYSTERESIS IN MTP

The purpose of coordinated controller is to smoothly start the engine and engage the wet clutch by coordinating the torque of motor and the torque of clutch. From the fitting results shown in Fig.3(d) and Fig.4(b), we can find that the mechanical hysteresis of clutch is much bigger than that of PMSM. Although the torque command given by coordinated controller is compatible, the actual torque may exhibit different dynamic characteristics because of the mechanical hysteresis. Thus, a coordinated controller which considers the influence of mechanical hysteresis is necessary for MTP. While it is a good choice to extend the PWA model with mechanical hysteresis, the increase in the number of dimensions always makes the solution difficult. Thus, this section proposed a hierarchical PWA-MSOF H_∞ control strategy as the coordinated controller of MTP. The upper layer controller is a PWA-based output-feedback H_∞ controller (PWA-SOF) which ensure the performance of MTP with ideal actuators; Different from the normal coordinated controllers which need to be individually designed for each stage, the performance index for PWA-based coordinated controller is unified for the discontinuous MTP system and the designed controller can ensure the stability

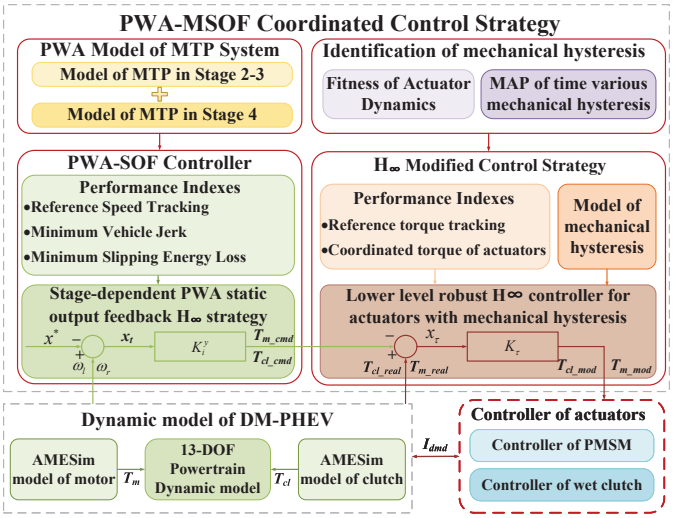

Fig. 5. Coordinated control architecture.

and optimality of the entire mode transition process. The lower layer controller is a state-feedback H_∞ controller to slove the mechanical hysteresis which may seriously deteriorate the performance of MTP and make a modification for the torque calculated by the proposed PWA-SOF controller. The combination of these two controllers is the PWA-MSOF control strategy which can deal with vehicle jerk caused by the discontinuous clutch engagement and mechanical hysteresis in MTP. The control architecture of PWA-MSOF is shown in Fig.5.

A. PWA-SOF controller for MTP without considering mechanical hysteresis

Based on the PWA model, a PWA-SOF control strategy for the MTP with discontinuous clutch engagement process is proposed.

According to [13], the SOF control strategy can be derived from a static state feedback (SSF) H_∞ controller. Thus, a static state feedback control strategy should be designed first. For the MTP of DM-PHEV, the PWA-SSF control law for MTP system in region i can be written as

$$u_t(k) = K_i x_t(k) \tag{24}$$

where K_i is the gain matrix in region i. Substituting Eq.(24) into Eq.(19), a closed loop system can be obtained as follows

$$\begin{cases} x_t(k+1) = \tilde{A}_i x_t(k) + E_i^d w(k) + b_i^d, z(k+1) = \tilde{C}_i x_t(k) \\ \tilde{A}_i = A_i^d + B_i^d K_i, \tilde{C}_i = C_i + D_i K_i \end{cases} \tag{25}$$

Then H_∞ performance index γ_∞ is defined as

$$\|z\|_2 \le {\gamma_\infty}^2 \|w\|_2 \tag{26}$$

It can be found that the PWA system formulates a switched system with the same equilibrium point. Based on the PWA system, the goal of H_∞ control strategy is to find Lyapunov function which not only ensure the stability of PWA system within one region, but also ensure the stability of system transmit from one region to another region. Thus, the MTP coordinated controller is to design a control gain K_i such that the MTP system is asymptotically stable and the H-infinity norm γ_i from w to z is minimized in the whole state region, as shown in Eq.(26).

Theorem 1. (Special case of [29]) For all $(i,j) \in \Theta$, if there exist matrices: $P_i = {P_i}^T > 0, P_j = {P_j}^T > 0, Y_i, W_i$ and scalar α_i, an optimal set of gains $K_i = W_i {Y_i}^{-1}$ in Eq.(31) exists such that the following LMIs hold:

$$\min_{\gamma^2, P_i, Y_i, W_i} \gamma^2 \tag{27}$$

if $i \in \Gamma_0$

$$\begin{bmatrix} P_i - Y_i - {Y_i}^T & * & * & * \\ 0 & -\gamma^2 I & * & * \\ A_i^d Y_i + B_i^d W_i & E_i & -P_j & * \\ C_i Y_i + D_i W_i & 0 & 0 & -I \end{bmatrix} < 0 \tag{28}$$

if $i \in \Gamma_1$

$$\begin{bmatrix} P_i - Y_i - {Y_i}^T & * & * & * & * \\ 0 & -\gamma^2 I & * & * & * \\ A_i^d Y_i + B_i^d W_i & E_i^d & \Psi_{ij} & * & * \\ C_i Y_i + D_i W_i & 0 & 0 & -I & * \\ H_i Y_i & 0 & \alpha_i h_i \left(b_i^d\right)^T & 0 & \Phi_i \end{bmatrix} < 0$$
$$\Psi_{ij} = -P_j - \alpha_i b_i^d \left(b_i^d\right)^T, \Phi_i = \alpha_i \left(I - h_i {h_i}^T\right) \tag{29}$$

where P_i is the Lyapunov matrix for $x_t(k)$; P_j is the Lyapunov matrix for $x_t(k+1)$; Specially, if $x_t(k)$ and $x_t(k+1)$ are in the same region, then $P_i = P_j$.

Proof. The proof is omitted here due to the limitation of space. The details can be found in reference [13], [29].

The controller will transfer the system states from the area not including the equilibrium point to the area including the equilibrium point as soon as possible and ensure the stability of the system during the switching process. Thus, compared with the regular model, the control strategy based on PWA system can acquire better performance during the transition from one region to another region, while ensuring the stability of whole system.

Finally, the optimal PWA state-feedback gain set K_i can be calculated in MATLAB by using LMI toolbox as

$$K_i = W_i {Y_i}^{-1} \tag{30}$$

Furthermore, the PWA static output feedback (PWA-SOF) control law can be described as

$$u_i(k) = K_i^y y(k) \tag{31}$$

Thus, the Eq.(19) can be transformed as

$$\begin{cases} x_t(k+1) = \hat{A}_i x_t(k) + E_i^d w(k) + b_i^d, z(k+1) = \hat{C}_i x_t(k) \\ \hat{A}_i = A_i^d + B_i^d K_i^y C_i^y, \hat{C}_i = C_i + D_i K_i^y C_i^y \end{cases} \tag{32}$$

According to [13], the design problem of the mode transition coordinated static output feedback controller can be equivalently not finding a set of output feedback gains K_i^y to satisfy $K_i^y C_i^y \triangleq K_i$. It can be known from Theorem 1 that $K_i = W_i {Y_i}^{-1}$, and then it can be seen that the problem can be transformed into finding a matrix transformation method for the result calculated based on the state feedback and writing it

in the form of multiplying the output feedback gain matrix by C_i^y. According to [13], based on the PWA static state feedback controller, the PWA static output feedback controller (PWA-SOF) of the MTP control system can be derived from Theorem 2 as follows.

Theorem 2. For Y_i and W_i in Theorem 1, make the following substitutions:

$$Y_i = Q_i Y_{Q,i} Q_i^T + R_i Y_{R,i} R_i^T, W_i = W_{R,i} R_i^T \tag{33}$$

where $Y_{Q,i} = {Y_{Q,i}}^T \in R^{(x-y)\times(x-y)}, Y_{R,i} = {Y_{R,i}}^T \in R^{y\times y}, W_{R,i} \in R^{u\times y}$ are new LMI variables. Q_i, R_i are constant matrices which satisfy that

$$C_i^y Q_i = \mathbf{0}, R_i = C_i^{y\dagger} + Q_i L_i, C_i^{y\dagger} = (C_i^y)^T \left(C_i^y (C_i^y)^T\right)^{-1} \tag{34}$$

If there exists feasible solutions for the substituted LMI, the PWA-SOF gains can be obtained as that:

$$K_i^y = W_{R,i} {Y_{R,i}}^{-1} \tag{35}$$

Variable Q_i can be selected as $Q_i = null\,(C_i^y)$. Variable $L_i \in R^{(x-y)\times y}$ and according to [30], the selection of L can be written as

$$L = Q_i^{\dagger} Y_i (C_i^y)^T \left(C_i^y Y_i (C_i^y)^T\right)^{-1} \tag{36}$$

where $Q_i^{\dagger} = \left((Q_i)^T Q_i\right)^{-1} (Q_i)^T$. This selection of L can ensure that the performance of the output feedback controller is closer to that of the state feedback controller.

Proof. The proof is omitted here due to the limitation of space. The details can be found in reference [30].

By substituting the variables in Theorem 1 and solving those LMIs, the output feedback control gain can be obtained according to Eq.(31).

B. Torque distribution of overdrive system

From the structure of DM-PHEV, we can find that the torque of motor 1 and motor 2 work together during the mode transition process, which can be described as an overdrive system. Since the MTP is a preparation process for the steady driving mode, the steady torque demand of hybrid mode is decided by the EMC. Thus here the torque T_{m1}^d, T_{m2}^d distributed by an EMC are considered as the reference torque to allocate the torque between motor 1 and motor 2. As the energy management controller is not the key issue in this paper, a simple rule-based energy management controller is adopted here. Quadratic optimal control strategy is adopted here to allocate the demand torque T_m from PWA-MSOF to torque of motor 1 T_{m1} and torque of motor 2 T_{m2}.

$$\min_u f_u = \frac{1}{2} \left\| Q_u \left(u - u_d\right) \right\|_2^2 \tag{37}$$

s.t.

$$\begin{aligned} u &= \begin{bmatrix} T_{m1} & T_{m2} \end{bmatrix}^T, u_d = \begin{bmatrix} T_{m1}^d & T_{m2}^d \end{bmatrix}^T \\ T_m &= \begin{bmatrix} \frac{1}{i_2} & 1 \end{bmatrix} \begin{bmatrix} T_{m1} \\ T_{m2} \end{bmatrix}, u_{\min} \le u \le u_{\max} \end{aligned} \tag{38}$$

C. Lower level robust H_∞ controller for actuators with mechanical hysteresis

Based on the mechanical hysteresis model built before, a lower level robust H_∞ controller is adopted here to modify the demand torque given by upper layer PWA-SOF controller.

The goal of this controller is to make the actual torque of actuators track the demand torque while the torque of clutch and motors can be coordinated during this process, the state variable of this system is selected as

$$x_\tau = \begin{bmatrix} T_{cl} - T_{cl\_dmd} & T_{m1} - T_{m1\_dmd} & T_{m2} - T_{m2\_dmd} \end{bmatrix}^T \tag{39}$$

where T_{cl_dmd} and T_{m_dmd} are the demand torque given by PWA-SOF.

Control inputs are defined as the difference between modified torque and demand torque given by PWA-SOF.

$$u_\tau = \begin{bmatrix} u_{cl} - T_{cl\_dmd} & u_{m1} - T_{m1\_dmd} & u_{m2} - T_{m2\_dmd} \end{bmatrix}^T \tag{40}$$

with u_m being the modified torque demand of motors, u_{cl} being the modified torque demand of clutch.

The goal of this controller is to modify the demand torque given by PWA-SOF so that the actual response torque of clutch and motors are coordinated. Thus, the performance output z_τ is selected as

$$\begin{aligned} z_\tau = \begin{bmatrix} T_{cl} - T_{cl\_dmd} & T_{m1} - T_{m1\_dmd} \\ T_{m2} - T_{m2\_dmd} & T_{cl} - i_2 T_m 2 - T_{m1} \end{bmatrix} \end{aligned} \tag{41}$$

The model of mechanical hysteresis can be described as

$$\dot{x}_\tau = A_\tau x_\tau + B_\tau u_\tau + E_\tau w_\tau \tag{42}$$

where

$$\begin{aligned} A_\tau &= \begin{bmatrix} -\frac{1}{\tau_{cl}} & 0 & 0 \\ 0 & -\frac{1}{\tau_{m1}} & 0 \\ 0 & 0 & -\frac{1}{\tau_{m2}} \end{bmatrix}, B_\tau = \begin{bmatrix} \frac{1}{\tau_{cl}} & 0 & 0 \\ 0 & \frac{1}{\tau_{m1}} & 0 \\ 0 & 0 & \frac{1}{\tau_{m2}} \end{bmatrix} \\ E_\tau &= \begin{bmatrix} 1 & 0 & 0 \\ 0 & 1 & 0 \\ 0 & 0 & 1 \end{bmatrix}, \begin{array}{l} \tau_{cl} \in \left[\tau_{cl}^{\min}, \tau_{cl}^{\max}\right] \\ \tau_m \in \left[\tau_m^{\min}, \tau_m^{\max}\right] \end{array} \end{aligned} \tag{43}$$

As the hysteresis parameter τ_{cl} and τ_m are time varying mechanical delays, defining

$$A_i = \begin{bmatrix} -\frac{1}{\tau_{cl}^i} & 0 & 0 \\ 0 & -\frac{1}{\tau_{m1}^i} & 0 \\ 0 & 0 & -\frac{1}{\tau_{m2}^i} \end{bmatrix}, B_i = -A_i \tag{44}$$

where

$$\tau_{cl}^i \in \left\{\tau_{cl}^{\max}, \tau_{cl}^{\min}\right\}, \tau_m^i \in \left\{\tau_m^{\max}, \tau_m^{\min}\right\} \tag{45}$$

Then the model can be transformed as

$$\begin{aligned} A\left(\lambda\right), B\left(\lambda\right) &= \sum_{i=1}^{8} \left(A_i, B_i\right)\lambda_i, \\ \lambda_i \ge 0, \sum_{i=0}^{8} \lambda_i &= 1; i = 1, \cdots, 8 \end{aligned} \tag{46}$$

Similarly, the Eq.(46) can be discretized as:

$$x_\tau\left(k+1\right) = A_\tau^d x_\tau\left(k\right) + B_\tau^d u_\tau\left(k\right) + E_\tau^d w_\tau\left(k\right) \tag{47}$$

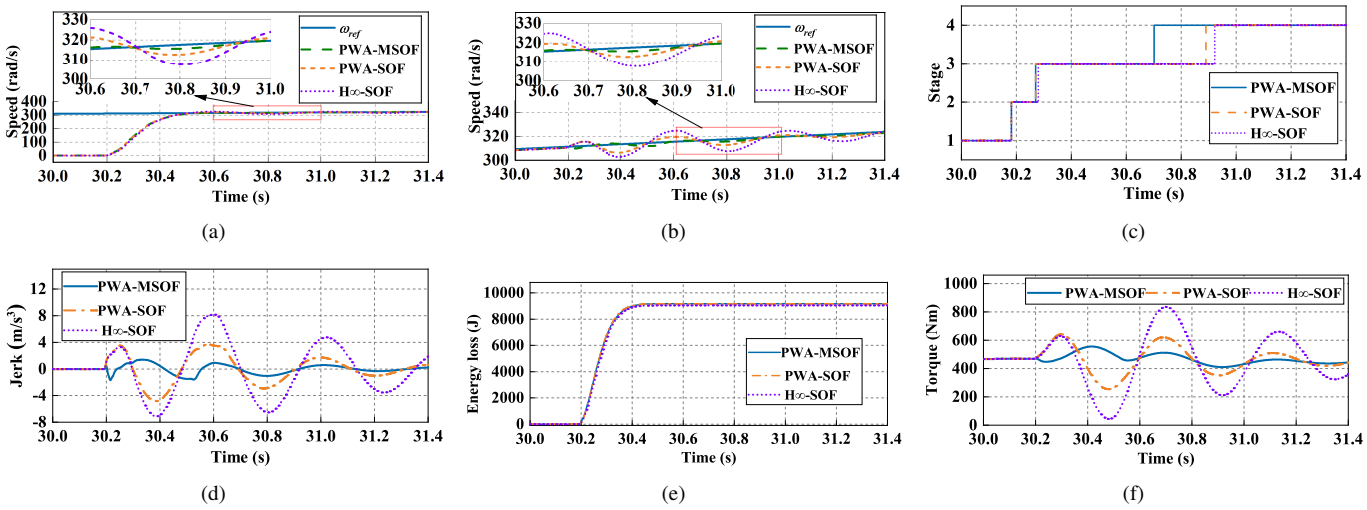

Fig. 6. Comparison of proposed PWA-MSOF, PWA-SOF and H_∞-SOF. **a** Comparison of clutch driven disc speed. **b** Comparison between clutch driving disc speed and reference speed. **c** Comparison of MTP stage. **d** Vehicle jerk. **e** Slipping energy loss. **f** Torque transmitted to the wheels.

Considering the uncertainties of mechanical hysteresis, a robust H_∞ controller is appropriate and practical. Therefore, a state feedback controller is designed as follows:

$$u_\tau = K_\tau x_\tau \tag{48}$$

For time-varying τ_{cl} and τ_m, find a Lyapunov matrix P_τ and control gain K_τ for Eq.(48), such that the closed-loop system Eq.(46) is asymptotically stable, the H_∞ norm γ_∞ from w_τ to z_τ is minimum. The control gain in Eq.(48) can be obtained through the following theorem.

Theorem 3. The control gain in Eq.(48) exists if there exists matrices P_τ, G_τ, Y_τ, such that the following LMI holds:

$$\begin{bmatrix} P_\tau - G_\tau - G_\tau^T & \mathbf{0} & A_\tau^d G_\tau + B_\tau^d Y_\tau & E_\tau^d \\ * & -I & C_\tau G_\tau + D_\tau Y_\tau & \mathbf{0} \\ * & * & -P_\tau & \mathbf{0} \\ * & * & * & -{\gamma_\infty}^2 I \end{bmatrix} < 0 \tag{49}$$

Proof. The proof is omitted here due to the limitation of space. The details can be found in reference [31].

Then the desired state-feedback gain K can be calculated in MATLAB by using LMI toolbox as

$$K_\tau = Y_\tau {G_\tau}^{-1} \tag{50}$$

Finally, the modification for the torque demand ΔT can be calculated as

$$\Delta T = K_\tau x_\tau \tag{51}$$

VI. Simulation and HiL Test Results

In this section, simulation and HiL tests will be done to verify the effectiveness of proposed PWA-MSOF controller.

A. Simulation and results analysis

To get insight into the performance of the PWA-MSOF, this paper will simultaneously show the simulations of the PWA-SOF without considering the mechanical hysteresis of actuators. Besides, an static output feedback H_∞ (H_∞-SOF) coordinated control strategy is also adopted here as a comparison with the upper layer PWA-SOF controller. The design of it can be found in [31]. The dynamic model of DM-PHEV is established in MATLAB/Simulink and AMESim according to the plant mode which can be found in the previous work [25]. The sampling intervals for plant model, upper layer controller and lower layer robust H_∞ controller are 10e-6 ms, 0.01 ms and 0.01 ms, respectively. The key parameters of this DM-PHEV are given in Table.II. The MTP from electric driving mode to hybrid driving mode usually happens in acceleration condition. Thus, here an acceleration scenario is adopted to verify the proposed coordinated control strategy.The feedback gain of upper layer PWA-SOF controller and lower layer robust H_∞ controller is:

$$\begin{aligned} K_1^y &= -\begin{bmatrix} -33.53 & -24.43 & -30.65 & -8.32 \\ -33.65 & -24.32 & -31.89 & -9.36 \end{bmatrix} \\ K_2^y &= \begin{bmatrix} 0 & -41.83 & -4.96 & 0.08 \\ 0 & -1.31 & -30.7 & -12.02 \end{bmatrix} \\ K_\tau &= \begin{bmatrix} -0.223 & 0.064 & 0.138 \\ 0.162 & -0.052 & -0.161 \\ 0.266 & -0.120 & -0.205 \end{bmatrix} \end{aligned} \tag{52}$$

The feedback gain of upper layer H_∞-SOF is:

$$\begin{aligned} K_1^y &= \begin{bmatrix} -28.85 & -21.53 & -17.54 & -0.69 \\ -29.37 & -22.19 & -21.94 & -2.13 \end{bmatrix} \\ K_2^y &= \begin{bmatrix} 0 & 0 & 0 & 0 \\ 0 & 0 & -15.10 & -4.88 \end{bmatrix} \end{aligned} \tag{53}$$

To verify the necessity of proposed PWA-MSOF, the results of PWA-MSOF,PWA-SOF and a H_∞-SOF controller working on DM-PHEV with mechanical hysteresis are shown in Fig.6. It can be seen from Fig.6(a) that both the speed of clutch driven disc ω_l controlled by PWA-SOF, PWA-MSOF and H_∞-SOF can track the reference speed. However, the ω_l controlled by PWA-MSOF can converge to the reference value faster and more smoothly. The speed of clutch driving disc ω_r which represents the vehicle speed is shown in Fig.6(b). Through the consideration of mechanical hysteresis, the ω_r controlled

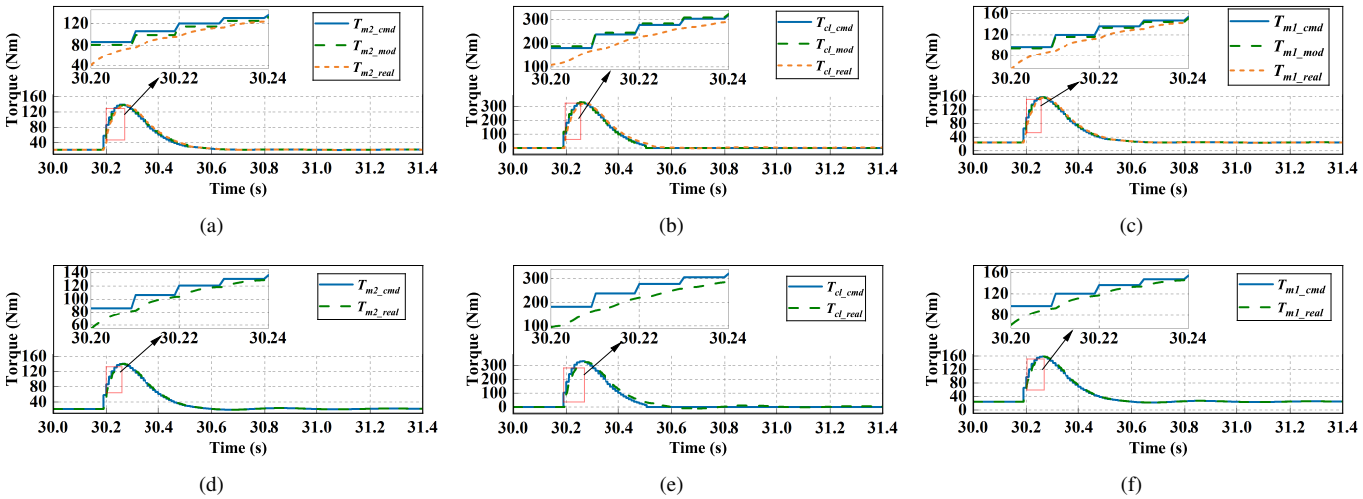

Fig. 7. Torque of actuators. **a** Actual and demand torque of motor 2 controlled by PWA-MSOF. **b** Actual and demand torque of clutch C1 controlled by PWA-MSOF. **c** Actual and demand torque of motor 1 controlled by PWA-MSOF. **d** Actual and demand torque of motor 2 controlled by PWA-SOF. **e** Actual and demand torque of clutch C1 controlled by PWA-SOF. **f** Actual and demand torque of motor 1 controlled by PWA-SOF.

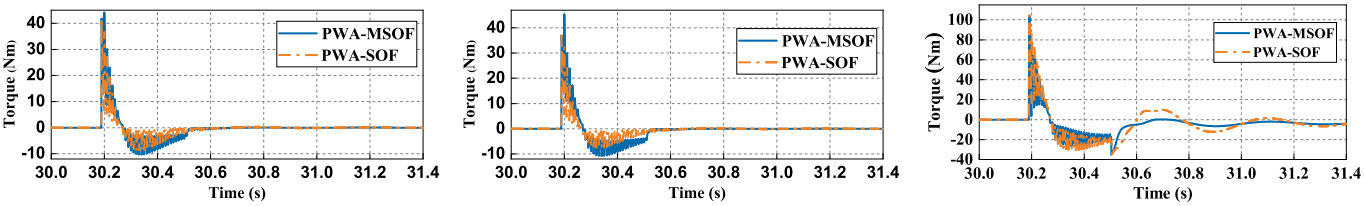

Fig. 8. Torque error between demand torque and actual torque of actuators. (a)Motor 1. (b)Motor 2. (c)Wet clutch.

TABLE II
PARAMETERS OF DM-PHEV

	Parameter	Value	Unit
Vehicle	Vehicle massm_{veh}	1970	kg
	Effective windward area A_a	2.66	m^2
	Wheel rolling radius R_w	0.353	m
	Wind resistance coefficient C_d	0.357	
	Rolling resistance coefficient f	0.016	
	Final reduction transmission ratio	3.842	
ICE	Maximum speed n_{emax}	5500	r/min
	Maximum output torque of T_{emax}	210	Nm
	Maximum output power P_{max}	63	Kw
Motor	Maximum power of motor 1 P_{1max}	55	Kw
	Maximumt torque of motor 1 T_{1max}	160	Nm
	Maximum speed of motor 1 n_{1max}	6200	r/min
	Maximum power of motor 2 P_{2max}	70	Kw
	Maximum torque of motor 2 T_{1max}	155	Nm
	Maximum speed of motor 2 n_{2max}	12000	r/min
Clutch	Number of clutch contact faces N	4	
	Oil density ρ	850	kg/m^3
	Outside radius of clutch plate R_o	180	mm
	Inside radius of clutch plate R_i	30	mm
	Piston diameter d_p	100	mm
	Rod diameter d_r	40	mm
	Oil pressure provided by the tank P_{in}	15	bar

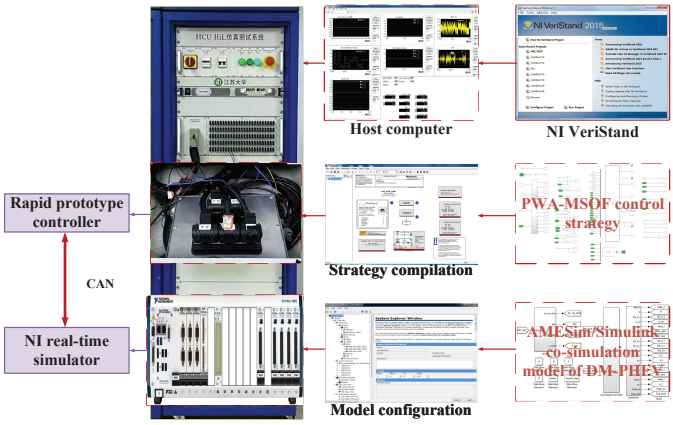

Fig. 9. Schematic diagram of HiL test.

by PWA-MSOF has fewer fluctuations than that controlled by PWA-SOF and H_∞-SOF controller. Besides, the speed controlled by the H_∞-SOF controller shows a larger fluctuation than that controlled by PWA-SOF, verifying that the PWA-SOF has better performance in dealing with the discontinuous dynamics caused by clutch engagement. Fig.6(c) denotes the current stage of MTP. At 30.2 s, a MTP command is given by the EMC. Then the MTP runs into Stage 2, engine start stage. The torque transmitted by clutch T_{cl} begins to increase to start the engine. Simultaneously, the torque of motor 1 and motor 2 rise to compensate the resistance torque from clutch C1. When the speed of engine exceeds engine idle speed, MTP runs into Stage 3, clutch slipping stage. When the speed difference is less than a certain value, MTP runs into Stage 4. We can find that the time of MTP controlled by PWA-MSOF

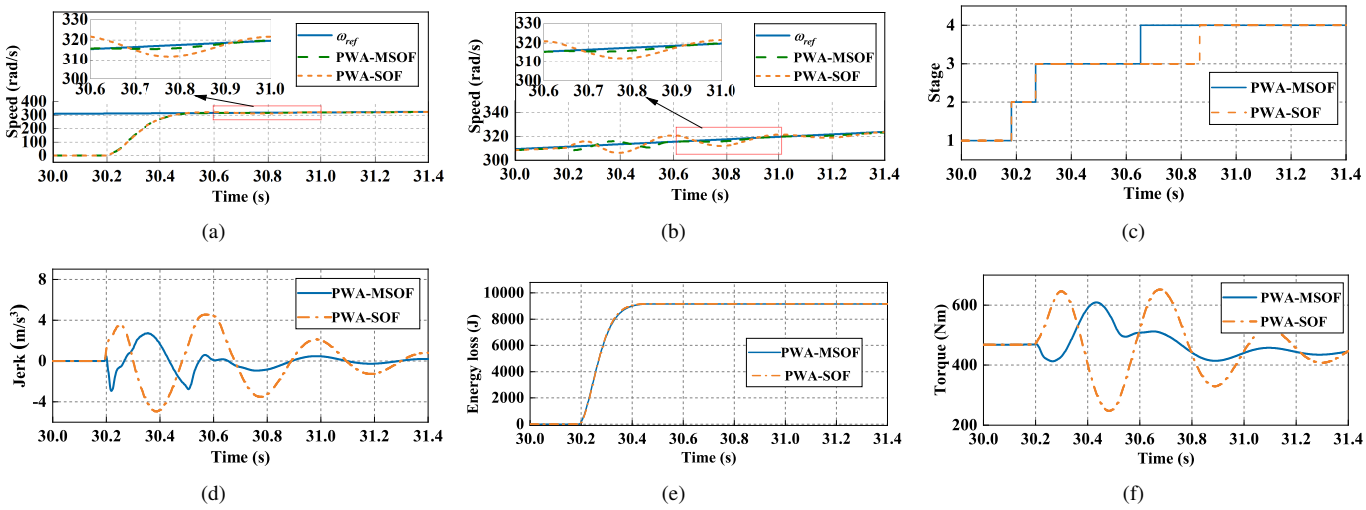

Fig. 10. Comparison of proposed PWA-MSOF and PWA-SOF in HiL test. **a** Comparison of clutch driven disc speed. **b** Comparison between clutch driving disc speed and reference speed. **c** Comparison of MTP stage. **d** Vehicle jerk. **e** Slipping energy loss. **f** Torque transmitted to the wheels.

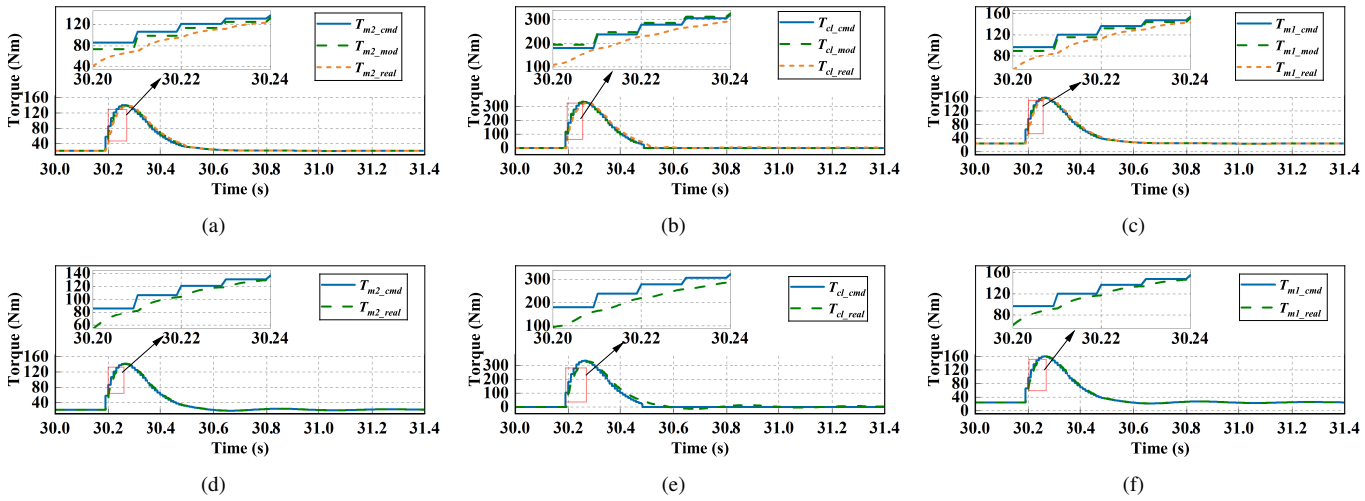

Fig. 11. Torque of actuators in HiL test. **a** Actual and demand torque of motor 2 controlled by PWA-MSOF. **b** Actual and demand torque of clutch C1 controlled by PWA-MSOF. **c** Actual and demand torque of motor 1 controlled by PWA-MSOF. **d** Actual and demand torque of motor 2 controlled by PWA-SOF. **e** Actual and demand torque of clutch C1 controlled by PWA-SOF. **f** Actual and demand torque of motor 1 controlled by PWA-SOF.

is 0.52 s, while that controlled by PWA-SOF and H_∞-SOF is about 0.71 s and 0.74 s, respectively. All the maximum vehicle jerk is smaller than recommended vehicle jerk (less than 10 $\mathrm{m/s^3}$). For H_∞-SOF controller, the maximum vehicle jerk is about 8.15 $\mathrm{m/s^3}$, which is much bigger than the other two controllers. As the PWA-SOF controller considered the global optimization during the MTP, while the H_∞-SOF controller can only optimize during the current stage of MTP. Thus, the MTP controlled by PWA-SOF exhibits smaller vehicle jerk at the border of clutch slipping stage and clutch engagement stage. The maximum vehicle jerk controlled by PWA-SOF reach to about 4.8 $\mathrm{m/s^3}$. This is caused by the uncoordinated dynamic characteristics of clutch and motors introduced by the mechanical hysteresis. While the proposed PWA-MSOF controller can effectively reduce the vehicle jerk to about 1.69 $\mathrm{m/s^3}$. At the same time, the slipping energy loss of these three controllers are similar. Thus, the proposed PWA-MSOF controller can acquire better performance of MTP with mechanical hysteresis.

From the performance indices, we can definitely find that the PWA-based controller exhibits better than traditional H_∞-SOF controller. To further verify the difference between proposed PWA-MSOF and PWA-SOF, the torque of actuators controlled by PWA-SOF and PWA-MSOF are shown in Fig.7. T_dmd is the ideal torque of actuators optimized by PWA-SOF. T_dmd_mod is the modified torque command given to the controller of actuators. The real torque response of actuators is T_real. It can be seen that compared with PWA-SOF, the demand torque of clutch is modified to be bigger so that the actual torque of actuators can be more closed to the demand torque. Since the response speed of motor is much quicker than clutch, to decrease the error between motors and clutch, the demand torque of motors are modified to be smaller. The torque errors between demand torque and actual torque

of actuators are shown in Fig.8(a), Fig.8(b) and Fig.8(c), respectively. While the torque error of the clutch is reduced, the torque error of the motor is increased to achieve torque coordination between the actuators. Based on the modified torque demand of PWA-MSOF, the torque transmitted to the wheels shows smaller fluctuations than that controlled by PWA-SOF as shown in Fig.6(f). Thus, the PWA-MSOF can make the actual torque of actuators coordinated through considering the mechanical hysteresis.

Totally, the proposed PWA-MSOF controller can effectively improve the performance of MTP with mechanical hysteresis introduced by actuators.

B. HiL test and results analysis

To verify the effectiveness, feasibility and real-time performance of proposed PWA-MSOF control strategy in the actual controllers and environment, the controller is implemented in a rapid prototyping controller and tested in real-time using a hardware-in-the-loop (HiL) simulator running a full nonlinear model. The nonlinear vehicle model built by AMESim is simulated in a NI real-time simulator which can simulate the dynamic characteristics of powertrain in high frequency. The control strategy (PWA-MSOF, PWA-SOF) is designed by MATLAB/Simulink and then be compiled and downloaded into the rapid prototype controller. The host computer can observe the data of HiL tests. The communication between rapid prototype controller and NI real-time simulator is realized by CAN bus. The schematic diagram of HiL test is shown in Fig.9.

As shown in Fig.10(a) and 10(b), the reference value of clutch speed ω_{ref} is well tracked by ω_l and ω_r controlled by PWA-MSOF. The fluctuation and tracking error of speed controlled by PWA-MSOF are smaller than those controlled by PWA-SOF. The quantitative results of performance indices of MTP are shown in Table III. In HiL test, the vehicle jerk controlled by PWA-SOF and PWA-MSOF is 4.9 and 2.32 $\mathrm{m/s^3}$, respectively. Compared with the former, the latter's value is reduced by 52.65%. Besides, the time of MTP controlled by PWA-MSOF is shorter than that controlled by PWA-SOF. The slipping energy loss of clutch controlled by the two methods is similar. Fig.11 shows the results of torque in HiL test. Totally, the test results are similar to the simulation results. Because of the noise of information transmission between controller and NI real-time simulator, the limitation of controller operation accuracy and speed and the CAN-induced delays, the results are a little different from those of simulation, but the trend is similar.

In short, the HiL test results verify the real-time performance of the proposed coordinated control strategy.

TABLE III
QUANTITATIVE COMPARISON RESULTS OF HIL.

Performance indices	PWA-SOF	PWA-MSOF
Jerk ($\mathrm{m/s^3}$)	4.9	2.32
Deviation of jerk	x	52.65%
Time (s)	0.698	0.495
Deviation of time	x	28.78%
Slipping energy loss (J)	9172	9170
Deviation of slipping energy loss	x	0.02%

VII. CONCLUSION

To suppress the influence of mechanical hysteresis and elevate the quality of MTP, a PWA-MSOF coordinated controller which can optimally allocate the torque of motor and clutch is proposed in this research. The main conclusions are shown the following:

1) The MTP with discontinuous clutch engagement process is described as a PWA system and a coordinated controller based on proposed PWA model of MTP is designed.
2) The mechanical hysteresis introduced by actuators are identified and robust H_∞ controller is adopted to eliminate the influence of uncoordinated mechanical hysteresis.
3) HiL test demonstrates that the vehicle jerk controlled by PWA-MSOF can be reduced by 52.65% with the PWA-MSOF strategy. Besides, the slipping energy loss and time of MTP of both controllers are similar.

In short, the proposed control strategy can improve the performance of MTP with mechanical hysteresis, and can provide a theoretical reference for the PHEV in engineering practice. Meanwhile, the proposed strategy is only validated in HiL test. In the future, a test bench with wet clutch and motors will be built and more tests about PWA-MSOF will be conducted.

ACKNOWLEDGMENT

This work is financially supported by National Natural Science Foundation of China [No. 52172358], Graduate Research and Innovation Program of Jiangsu province [KYCX21_3330], Six Talent Peaks Project in Jiangsu Province (CN) [No. JXQC-036], the China Scholarship Council [NO.202008690006, 201908320221].

REFERENCES

[1] W. Zhou, N. Zhang, and H. Zhai, "Enhanced battery power constraint handling in mpc-based hev energy management: a two-phase dual-model approach," *IEEE Transactions on Transportation Electrification*, vol. 7, no. 3, pp. 1236–1248, 2021.
[2] C. Liang, X. Xu, F. Wang, and Z. Zhou, "H_∞ non-clutch coordinated control for mode transition system of dm-phev with can-induced delays," *Nonlinear Dynamics*, vol. 107, no. 1, pp. 1003–1021, 2022.
[3] Z. Zhao, L. Jiang, C. Wang, and M. Li, "Engine start-up optimal control for a compound power-split hybrid powertrain," *Mechanical Systems and Signal Processing*, vol. 120, pp. 365–377, Apr. 2019.
[4] Y. Liu, D. Chen, Z. Lei, D. Qin, Y. Zhang, R. Wu, and Y. Luo, "Modeling and control of engine starting for a full hybrid electric vehicle based on system dynamic characteristics," *International Journal of Automotive Technology*, vol. 18, pp. 911–922, 2017.
[5] C. Yang, X. Jiao, L. Li, Y. Zhang, and Z. Chen, "A robust h-infinity control-based hierarchical mode transition control system for plug-in hybrid electric vehicle," *Mechanical Systems and Signal Processing*, vol. 99, pp. 326 – 344, 2018.
[6] S. Zhou, P. Walker, Y. Tian, and N. Zhang, "Mode switching analysis and control for a parallel hydraulic hybrid vehicle," *Vehicle System Dynamics*, vol. 0, pp. 1–21, 2020.
[7] D. Xu, J. Zhang, B. Zhou, and H. Yu, "Investigation of mode transition coordination for power-split hybrid vehicles using dynamic surface control," *Proceedings of the Institution of Mechanical Engineers, Part K: Journal of Multi-body Dynamics*, vol. 233, no. 3, pp. 696–713, 2019.

[8] F. Wang, J. Xia, X. Xu, Y. Cai, Z. Zhou, and X. Sun, "New clutch oil-pressure establishing method design of phevs during mode transition process for transient torsional vibration suppression of planetary power-split system," *Mechanism and Machine Theory*, vol. 148, p. 103801, 2020.

[9] C. Liang, X. Xu, F. Wang, and Z. Zhou, "Coordinated control strategy for mode transition of dm-phev based on mld," *Nonlinear Dynamics*, vol. 103, no. 1, pp. 809–832, 2021.

[10] S. Song, Y. Guan, Z. Fu, and H. Li, "Switching control from motor driving mode to hybrid driving mode for phev," in *2017 Chinese Automation Congress (CAC)*, 2017, pp. 4209–4214.

[11] A. Benine-Neto and S. Mammar, "Piecewise affine state feedback controller for lane departure avoidance," in *2011 IEEE Intelligent Vehicles Symposium (IV)*, 2011, pp. 839–844.

[12] Y. Gao, "Application research of piecewise affine theory in vehicle anti-lock brake system," in *Proceedings of the 32nd Chinese Control Conference*, 2013, pp. 609–614.

[13] J. Wu, H. Zhou, and Z. Liu, "Practical static output feedback control methods for constrained piecewise affine systems: An application in vehicle suspension control," in *2019 IEEE International Symposium on Circuits and Systems (ISCAS)*, 2019, pp. 1–5.

[14] J. Wu, Z. Liu, and W. Chen, "Design of a piecewise affine h_∞ controller for mr semiactive suspensions with nonlinear constraints," *IEEE Transactions on Control Systems Technology*, vol. 27, no. 4, pp. 1762–1771, 2019.

[15] S. Cheng, L. Li, C.-Z. Liu, X. Wu, S.-N. Fang, and J.-W. Yong, "Robust lmi-based h-infinite controller integrating afs and dyc of autonomous vehicles with parametric uncertainties," *IEEE Transactions on Systems, Man, and Cybernetics: Systems*, vol. 51, no. 11, pp. 6901–6910, 2020.

[16] C. F. Caruntu, A. E. Balau, M. Lazar, P. P. Bosch, and S. Di Cairano, "Driveline oscillations damping: A tractable predictive control solution based on a piecewise affine model," *Nonlinear Analysis: Hybrid Systems*, vol. 19, pp. 168–185, 2016.

[17] J. Kang, X. Li, Y. Liu, S. Mu, and S. Wang, "Predictive current control with torque ripple minimization for pmsm of electric vehicles," in *2018 IEEE International Power Electronics and Application Conference and Exposition (PEAC)*, 2018, pp. 1–6.

[18] H. Wei, J. Yu, Y. Zhang, and Q. Ai, "High-speed control strategy for permanent magnet synchronous machines in electric vehicles drives: Analysis of dynamic torque response and instantaneous current compensation," *Energy Reports*, vol. 6, pp. 2324–2335, 2020.

[19] M. S. Rahmat, F. Ahmad, A. K. M. Yamin, V. R. Aparow, and N. Tamaldin, "Modelling and torque tracking control of permanent magnet synchronous motor for hybrid electric vehicles," *International Journal of Automotive and Mechanical Engineering*, vol. 7, p. 955, 2013.

[20] P. D. Walker, B. Zhu, and N. Zhang, "Nonlinear modeling and analysis of direct acting solenoid valves for clutch control," *Journal of dynamic systems, measurement, and control*, vol. 136, no. 5, p. 051023, 2014.

[21] J. Park, S. Choi, J. Oh, and J. Eo, "Adaptive slip engagement control of a wet clutch in vehicle powertrain based on transmitted torque estimation," *Mechanical Systems and Signal Processing*, vol. 171, p. 108861, 2022.

[22] Y. Liu, D. Chen, Z. Lei, D. Qin, Y. Zhang, R. Wu, and Y. Luo, "Modeling and control of engine starting for a full hybrid electric vehicle based on system dynamic characteristics," *International Journal of Automotive Technology*, vol. 18, no. 5, pp. 911–922, 2017.

[23] Y. Yang, Y. He, Z. Yang, C. Fu, and Z. Cong, "Torque coordination control of an electro-hydraulic composite brake system during mode switching based on braking intention," *Energies*, vol. 13, no. 8, 2020.

[24] J. Gao, D. Lou, and T. Zhang, "Optimized control of dynamical engine-start process in a hybrid electric vehicle," SAE Technical Paper, Tech. Rep., 2020.

[25] C. Liang, X. Xu, and F. Wang, "Mld based model and validation of dm-phev in mode transition process," in *2021 40th Chinese Control Conference (CCC)*. IEEE, 2021, pp. 1405–1412.

[26] J. Wu, H. Zhou, Z. Liu, and M. Gu, "A load-dependent pwa-h-infinity controller for semi-active suspensions to exploit the performance of mr dampers," *Mechanical Systems and Signal Processing*, vol. 127, pp. 441–462, 2019.

[27] J. Wu and Z. Liu, "Piecewise affine h-infinity control of half-car magneto-rheological suspension systems," *IFAC-PapersOnLine*, vol. 51, no. 31, pp. 967–972, 2018.

[28] K. Suman and A. T. Mathew, "Speed control of permanent magnet synchronous motor drive system using pi, pid, smc and smc plus pid controller," in *2018 International Conference on Advances in Computing, Communications and Informatics (ICACCI)*, 2018, pp. 543–549.

[29] Y. Gao and Z. Liu, "Lmi-based h-infinity control scheme for discrete-time piecewise affine systems," *Proceedings of the World Congress on Intelligent Control and Automation (WCICA)*, 01 2008.

[30] F. Palacios-Quiñonero, J. Rubió-Massegú, J. M. Rossell, and H. R. Karimi, "Feasibility issues in static output-feedback controller design with application to structural vibration control," *Journal of the Franklin Institute*, vol. 351, no. 1, pp. 139–155, 2014.

[31] C. Liang, X. Xu, F. Wang, S. Wang, and Z. Zhou, "Can-induced asynchronous random delays-considered mode transition system for dm-phev based on constrained output feedback robust control strategy," *IEEE Transactions on Vehicular Technology*, 2022.

Cong Liang was born in Funing, China, in 1997. She received the B.S. Degree in vehicle engineering from Jiangsu University. She is currently working toward the Ph.D. degree in vehicle engineering at the Automotive Engineering Research Institute, Jiangsu University.

Xing Xu was born in Haian, China, in 1979. He received the Ph.D. degree in agricultural electrification and automation from Jiangsu University, Zhenjiang, China, in 2010. Since 2010, he has been with the Automotive Engineering Research Institute, Jiangsu University, where he is currently a Professor. His research interests are in electric and hybrid-electric vehicles, energy storage systems, advanced suspension system.

Daniel J. Auger (M'13-SM'15) was born in Rainham, U.K., in 1977. He received the M.Eng. and Ph.D. degrees from the University of Cambridge, Cambridge, U.K., in 2000 and 2005, respectively.

From 2004 to 2008, he was a Senior Engineer with BAE Systems, U.K. From 2008 to 2013, he was a Senior Consultant with MathWorks, U.K. He joined the Advanced Vehicle Engineering Centre, Cranfield University, Cranfield, U.K., in 2013, and is currently Reader in Electrification, Automation and Control. His battery-related research interests include hybrid energy storage systems, state estimation, and electrical/thermal modeling. He also has a general interest in applications of modeling and control to vehicle systems, including driving automation and advanced driver-assistance systems (ADAS).

Dr. Auger is a former Chair of the IEEE U.K. & Ireland Control Systems Society Chapter, an IET Fellow, and a Chartered Engineer.

Feng Wang received his PhD in vehicle engineering from Northwestern Polytechnical University, Xi'an, China, in 2014. He is currently an associate professor of vehicle engineering and a member of automotive engineering research laboratory at the Automotive Engineering Research Institute, Jiangsu University, China.His research interests focuses on transient vibration characteristics of hybrid planetary coupling transmission system.

Shaohua Wang He received the Ph.D. degree in Automotive Engineering from Jiangsu University, Zhenjiang, China, in 2013. Since 2020, he has been with the Automotive Engineering Research Institute, Jiangsu University, where he is currently a Professor. His research interests are in electric and hybrid-electric vehicles, vehicle system dynamics and vehicle dynamic performance simulation and control.